

Design-principles of cell circuits with paradoxical components – Supporting Information

Yuval Hart^a, Yaron E. Antebi^b, Avraham E. Mayo^a, Nir Friedmann^b and Uri Alon^a

^aDepartment of Molecular Cell Biology, ^bDepartment of Immunology, Weizmann Institute of Science, Rehovot Israel 76100

Contents

General model with one cell type and one ligand.....	1
General model with two cell types, a progenitor cell and its differentiated form interacting with one ligand.....	5
Experimental evidences for insensitivity of differentiated cells to precursors initial levels	8
Theoretical studies on homeostasis and differentiation processes in the immune system	10
Fold change detection in the differentiation process of CD4+ to iTregs and Th17.....	12
An approximate analytical solution of the stereotyped pulse of the IL-27 circuit.....	13
Stability analysis of the stereotyped pulse (IL-27) circuit with and without a constant production from a differentiation process.....	14
General model of robust stereotyped pulse response.....	15

General model with one cell type and one ligand

Here we study the class of circuits with one cell type and one ligand. We find that this class of circuits can show a stable steady-state cell level that is reached for a wide range of initial conditions. This results from integral feedback that is inherent to the circuit topology. A second stable OFF state is achieved when the ligand is pleiotropic. Finally, we discuss the effects of non-linear terms on the steady-state solutions and their stability.

We begin with a general model: cells can proliferate and be removed at rates $\beta(c)$, $\alpha(c)$ respectively. The ligand, c , is produced by the cells at a rate $\beta_2 X$ and/or constitutively by external sources (e.g. by antigen presenting cells (APC)) at rate β_3 . The ligand may be removed by degradation at a rate $\gamma(c)$ and/or by uptake (endocytosis) by the cells at a rate $\alpha_0 X f(c)$. The functions $f(c)$, $\gamma(c)$ are smooth,

differentiable and monotonic increasing functions (e.g. linear, Michaelis-Menten or Hill functions)

$$(S1) \quad \dot{X} = (\beta(c) - \alpha(c))X$$

$$(S2) \quad \dot{c} = \beta_3 + \beta_2 X - \alpha_0 X f(c) - \gamma(c)$$

For the existence of a non-zero fixed point, two conditions must be met: First, $\beta(c), \alpha(c)$ must intersect (so that $dX/dt=0$), such that

$$(S3) \quad \exists c^* > 0: \beta(c^*) = \alpha(c^*)$$

Second, exists a positive cell level, $X^*>0$, at which $dc/dt=0$, namely:

$$(S4) \quad X^* = \frac{\beta_3 - \gamma(c^*)}{\alpha_0 f(c^*) - \beta_2} > 0$$

When these two conditions apply, the steady state solution $X=X^*$ is reached for a wide range of initial levels (all levels within the basin of attraction of that fixed point, see Fig. S1). Furthermore, X^* levels can be tuned by ligand secretion from external sources (the parameter β_3).

For the stability of the fixed points we analyze the Jacobian of the dynamical system of Eqs. (S1,S2) and derive the constraints on the functions for stability (for simplicity, we assume next $\gamma(c) = \gamma c$, which does not change the qualitative conclusions):

$$(S5) \quad J = \begin{pmatrix} \beta(c) - \alpha(c) & (\beta'(c) - \alpha'(c))X \\ \beta_2 - \alpha_0 f(c) & -\alpha_0 X f'(c) - \gamma \end{pmatrix}$$

Assuming that $f(0)=0$, and demanding that $\text{Det}(J)>0$ and $\text{Tr}(J)<0$ one finds conditions on the stability of the following points:

1. $X = 0, c = \frac{\beta_3}{\gamma} = c_0$: The point is stable when $-(\beta(c_0) - \alpha(c_0))\gamma > 0$ and $\beta(c_0) - \alpha(c_0) - \gamma < 0$ which yields the condition $\beta(c_0) < \alpha(c_0)$. When $\beta_3 = 0$ then, one has $c_0 = 0$ and the condition sets production to be lower than degradation at the zero concentration point, making the OFF state stable.
2. $X = X^*, c = c^*$: Since the trace of J is always negative, the only condition for stability is that the determinant be positive: $-(\beta'(c^*) - \alpha'(c^*))(\beta_2 - \alpha_0 f(c^*)) > 0$ which means that either $\beta'(c^*) > \alpha'(c^*)$ and $\beta_2 < \alpha_0 f(c^*)$ or $\beta'(c^*) < \alpha'(c^*)$ and $\beta_2 > \alpha_0 f(c^*)$. Thus, the system is stabilized either by ligand uptake being larger than ligand production by X or by ligand induced removal rate being larger than ligand induced proliferation rate at c values larger than c^* .

In order to have both an ON state and an OFF state, the monotonic rates $\beta(c), \alpha(c)$ need to cross each other at least twice, this can only happen if the ligand affects both rates. Thus, the ligand must be paradoxically pleiotropic in order to have stable ON and OFF states.

The presented analysis can be applied to cases where there are a higher number of crossing points between $\beta(c)$ and $\alpha(c)$ to obtain several fixed points in the positive quadrant and to cases where the dynamic equation for X is generalized to: $\dot{X} = (\beta(c) - \alpha(c))g(X)$ as long as $g(X)$ is a monotonic increasing function and $g(0) = 0$.

These considerations show that, for a wide range of functional forms of the interactions, these topological circuits yield stable ON and OFF states. To illustrate this, we plot the phase space of all of the 15 out of the 24 topological circuits which have a stable ON state (see Fig. 3 in the main text), including nullclines and dynamics, using the following set of functions $\alpha(c) = 1 + c$, $\beta(c) = \frac{c^2}{1+c^2}$ and $f(c) = \frac{c}{c+1}$ (see Fig. S1).

Four circuits out of the 15 yield both ON and OFF states and another four circuits yield a pulse in ligand levels before converging to the stable ON state (of which one circuit is in common with the previous four topologies, see Fig. S1). In all of these circuit topologies the ligand is paradoxically pleiotropic.

The dynamic behavior of the pleiotropic topological circuits (7 in number) is set by the X and c relationship dictated by the ligand nullcline ($dc/dt=0$, see Eq. (S4)) – if $X(c)$ is a monotonic increasing function of ligand levels, then the circuit has two stable states, ON and OFF. If $X(c)$ is a monotonic decreasing function of ligand levels, the circuit has a stable ON state that is reached after a pulse in ligand levels (when cell levels and ligand levels are assumed to be at low levels initially).

We next discuss the case where there are also non-linear terms in X, limiting cell (X) growth. We show that a small perturbation of non-linear terms of order ϵ adds small corrections of order ϵ to the fixed point. We further specify the limitations set on the perturbations to maintain the stability of the fixed points.

The set of dynamic equations is

$$(S6) \quad \dot{X} = (\beta(c) - \alpha(c))X - \epsilon q(c) h(X)$$

$$(S7) \quad \dot{c} = \beta_3 + \beta_2 X - \alpha_0 X f(c) - \gamma c$$

Where $h(X)$ is a differentiable monotonically increasing function of X . Analysis shows that solutions of the above equations are shifted by an order of ϵ away:

$$(S8) \quad X_{st}^{(1)} = X_{st}^{(0)} + \epsilon X_{st}^{(1)}$$

$$(S9) \quad c_{st}^{(1)} = c_{st}^{(0)} + \epsilon c_{st}^{(1)}$$

for the point $X=0$, the new solutions are shifted by

$$(S10) \quad X_{st}^{(1)} = \frac{q(c_0)h(0)}{\beta(c_0) - \alpha(c_0)}$$

$$(S11) \quad c_{st}^{(1)} = \frac{1}{\gamma}(\beta_2 - \alpha_0 f(c_0)) \frac{q(c_0)h(0)}{\beta(c_0) - \alpha(c_0)}$$

Note that the shifts are both zero if $h(X) = X^n$ (i.e. $h(0)=0$, as in the logistic correction:

$\beta(c)X \rightarrow \beta(c)X(1 - \frac{X}{X_{max}})$). When considering the robust non-zero fixed point

$(X = X^*, c = c^*)$, the corrections are:

$$(S12) \quad X_{st}^{(1)} = \frac{q(c_{st}^{(0)})h(X_{st}^{(0)})(\gamma + \alpha_0 X_{st}^{(0)} f'(c_{st}^{(0)}))}{X_{st}^{(0)} (\beta'(c_{st}^{(0)}) - \alpha'(c_{st}^{(0)}))(\beta_2 - \alpha_0 f(c_{st}^{(0)}))}$$

$$(S13) \quad c_{st}^{(1)} = \frac{q(c_{st}^{(0)})h(X_{st}^{(0)})}{X_{st}^{(0)} (\beta'(c_{st}^{(0)}) - \alpha'(c_{st}^{(0)}))}$$

We next analyze the shifted fixed points stability. The Jacobian of the system is:

$$(S14) \quad J = \begin{pmatrix} \beta(c) - \alpha(c) - \epsilon q(c)h'(X) & (\beta'(c) - \alpha'(c))X - \epsilon q'(c)h(X) \\ \beta_2 - \alpha_0 f(c) & -\alpha_0 X f'(c) - \gamma \end{pmatrix}$$

Assuming $h(X)$ is a polynomial (with powers $n \geq 2$), the following conditions of stability should hold for the following points:

- (1) $X = 0, c = c_0$: Conditions for stability are the same, i.e. $\beta(c_0) < \alpha(c_0)$.
- (2) $X = X^*, c = c^*$: The stability of this point may be dependent on the form of $h(X)$ since bifurcation can arise even for small values of ϵ . Below we list the conditions where the fixed point remains stable (for brevity we denote $g(c) = \beta(c) - \alpha(c)$). We denote the determinant as $D = d_0 + \epsilon d_1$ and the trace $T = -t_0 + \epsilon t_1$ and assume that the unperturbed determinant and trace hold the stability constraints, i.e. $d_0 > 0$ and $t_0 < 0$. We obtain the following conditions on the dynamic functions:

$$\frac{h(X_0)q(c_0)(t_0 + \gamma)}{d_0 X_0} + \frac{h(X_0)q'(c_0)}{X_0 g'(c_0)} - \left(\frac{t_0}{d_0} q(c_0)h'(X_0) + \frac{h(X_0)q(c_0)g''(c_0)}{X_0 g'(c_0)^2} \right) < \frac{1}{\epsilon} \quad \&$$

$$\frac{h(X_0)(t_0^2 + d_0)}{d_0 t_0 X_0} - \left(\frac{\gamma}{d_0 X_0} h(X_0) + \frac{h'(X_0)}{t_0} + \frac{h(X_0) \alpha_0 f''(c_0)}{t_0 g'(c_0)} \right) < \frac{1}{\epsilon q(c_0)}$$

Specifically, when $h(X) \sim X^2$ (as in the logistic term described above), the shifts in the

fixed point are: $X_{st}^{(1)} = \frac{X_{st}^{(0)} q(c_{st}^{(0)}) (\gamma + \alpha_0 X_{st}^{(0)} f'(c_{st}^{(0)}))}{g'(c_{st}^{(0)}) (\beta_2 - \alpha_0 f(c_{st}^{(0)}))}$ and $c_{st}^{(1)} = \frac{q(c_{st}^{(0)}) X_{st}^{(0)}}{g'(c_{st}^{(0)})}$.

For example, for the case of no endocytosis of c by X (*i.e.* $\alpha_0 = 0$) and a linear X dependence of cytokine secretion (such as the case discussed in the main text) the shifts are approximately linear in the fixed point value of X^* . For this specific biological case the stability of the shifted fixed point is maintained whenever $\text{Det}(J) > 0$ ($\text{Tr}(J)$ is always negative), meaning:

$g'(c_{st}^{(0)}) < X_{st}^{(0)} \epsilon q(c_{st}^{(0)}) \left(\frac{q'(c_{st}^{(0)})}{q(c_{st}^{(0)})} - \frac{g''(c_{st}^{(0)})}{g'(c_{st}^{(0)})} \right)$. This condition is likely to be met

if one assumes that ϵ is small enough and $\beta(c), \alpha(c)$ are smooth enough since stability of the system without non-linear perturbations is achieved

when: $g'(c_{st}^{(0)}) = \beta'(c_{st}^{(0)}) - \alpha'(c_{st}^{(0)}) < 0$.

We therefore conclude that adding a non-linear perturbation of order ϵ to the dynamic equation that acts to limit cell population will shift the fixed-point values by an order of ϵ and may not affect the stability of that point.

General model with two cell types, a progenitor cell and its differentiated form interacting with one ligand

In this section we treat the class of circuits with two cells populations, progenitor and differentiated cells interacting with a single ligand. We use general functional forms for the interactions between the circuit's components, and characterize the underlying mechanism for robust differentiated cell levels which are independent of progenitor cell amounts. We also scan circuit topologies to analytically find prototypical robust circuits, map the conditions for their robustness and list possible realizations of these circuits.

We start by presenting the class of circuits with two cell types and a single ligand:

The progenitor cells X_0 , differentiate to cell type X_1 which may proliferate or be removed. The ligand, c , can effect cell differentiation, cell proliferation and/or cell death either by activating or inhibiting each reaction. The ligand can be produced

constitutively, or by either cell type (X_0 or X_1) and be removed either by degradation or by uptake by either cell type (X_0 or X_1). The general set of dynamic equations is given by (see Fig. S2, Inset)

$$(S15) \quad \dot{X}_1 = \beta_0(X_0, c) + (\beta(c) - \alpha(c))X_1$$

$$(S16) \quad \dot{c} = \beta_3 + \beta_1(X_0, c) + \beta_2(X_1, c) - \alpha_1(c)X_0 - \alpha_2(c)X_1 - \gamma c$$

The circuits differ by the terms that are present in that specific circuit topology. We find that there are 280 circuits which are ‘connected’, in the sense that the ligand and cells affect each other.

A sufficient condition for these circuit topologies to exhibit robustness of differentiated cells to progenitor levels ($\frac{dX_{1, st}}{dX_0} = 0$) is that the system has an integral feedback mechanism. Then, the condition for robustness is that the system shows a stable non-zero fixed point, and that there exists a transformation $q = h(X_1, c, X_0)$ such that

$$(S17) \quad \dot{q} = w(q)b(X_1)$$

That is, \dot{q} incorporates the integral feedback mechanism on X_1 . In this case one can define a new variable,

$$(S18) \quad z = \int_0^q \frac{ds}{w(s)}$$

which will yield an integral feedback equation for X_1

$$(S19) \quad \dot{z} = b(X_1)$$

$$(S20) \quad \dot{X}_1 = f_1(X_0, X_1, c(X_1, z)) - g_1(X_1, c(X_1, z))$$

If $b(X_1)$ has a unique zero $b(X_1^*) = 0$ then at steady-state, $X_1 = X_1^*$ and this value does not depend on X_0 , the level of progenitor cells, since X_0 does not affect the function $b(X_1)$. There is no other way to obtain a fixed point, because the function $b(X_1)$ is nonzero, and hence dz/dt is nonzero, unless $X_1 = X_1^*$. This way, an integral feedback mechanism (1–3) assures that differentiated cell levels are kept independent of progenitor cell amounts.

We next asked which circuit topologies show robustness to progenitor cell concentrations. We find five classes of circuit topologies, each containing several topologies, which yield robustness to progenitor cell levels (see Table S1). All of

these circuits exhibit an integral feedback mechanism as analyzed in Eq. S19-S20. Four of these circuit classes contain several constraints on the allowed interactions between the two cell types and the ligand (e.g. linear uptake or secretion of ligand by cells). However, since these are only general characteristics of a large possible equivalence class, many biological circuits may be realized for each such prototypical circuit. These circuits and their possible realizations are listed in Table S1. Of particular interest is the circuit where robustness is achieved with only the assumption that signaling (X_0 differentiation to X_1) has the same functional dependence on c as ligand uptake by X_0 (meaning $\beta_0(X_0, c) = \beta_0 X_0 f(c)$ and $\alpha_1(c)X_0 = \alpha_1 X_0 f(c)$ where $f(c)$ is the same for both interactions). This is the case discussed in the main text: endocytosis and signaling often use the same receptors, and thus are linked biological processes. In this case, no further restriction on the functional form of all other reactions is necessary, since the transformed variable z is given by

$$(S21) \quad z = \alpha_1 X_1 + \beta_0 c \rightarrow \dot{z} = \alpha_1(\beta - \alpha)X_1 + \beta_0(\beta_3 + \beta_2(X_1)) = b(X_1)$$

making it a robust design that is insensitive to progenitor levels by an integral feedback mechanism.

To illustrate this, we plot the phase space of the 17 out of the 280 topological circuits (see Fig. 3b in the main text), including nullclines and dynamics using the following set of functions $\alpha(c) = 1 + c$, $\beta(c) = \frac{c^2}{1+c^2}$ and $f(c) = \frac{c}{c+1}$ and with two levels of precursor cells X_0 , $X_0=1$ (blue) and $X_0=2$ (green) (see Fig. S2). Indeed, the 4 circuits which are predicted to be insensitive to X_0 levels show that while the nullcline crossing point changed in terms of c levels, X levels stayed the same (Fig. S2). This indicates that ligand levels ‘buffer’ X levels when X_0 levels change. We also find another class of circuit topologies (e.g. circuit design 13 in Fig S2, marked with an asterisk) in which steady-state ligand levels are insensitive to X_0 levels. These stem from a similar integral feedback mechanism but on the dynamic variable c , ligand levels.

Experimental evidences for insensitivity of differentiated cells to precursors initial levels

In the following section we describe experimental evidences from several previous studies done with adoptive transfer models indicating insensitivity of effector/differentiated cells to precursor initial levels. The studies listed below show that while precursor levels are varied over a range of 3-4 orders of magnitude, effector cells levels varies by less than an order of magnitude.

The studies and their findings are listed below:

1. Whitmire et al (4): Precursor frequency, Nonlinear proliferation and functional maturation of virus specific CD4 T-cells:

Whitmire et. al. use an adoptive transfer model to measure expansion and proliferation of transferred and endogenous cells. They find that there is saturation of the expansion at the very high range of precursor levels. More interestingly, on the lower, more physiological regime of precursor frequency, total expansion of cells changes by about half an order of magnitude, while adoptive transfer cell levels increase by more than 3 orders of magnitude (Fig. 2B in their paper).

2. Quiel et al.(5): Antigen stimulated CD4 T-cell expansion is inversely and log-linearly related to precursor number:

Quiel et al quantify the factor of expansion (FE) of different levels of inactivated adoptively transferred cells. They find an inverse, linear connection between $\log(\text{FE})$ and $\log(\text{initial number of precursor cells})$ with slope -0.5. This indicates that the final cell number goes like $n_{\text{day } 8} \propto n^{0.5}$. They find no correlation of FE decrease with precursor levels to IL-2, IFN-gamma, FAS, IL-7, IL-15 or Tregs. A model of a delayed negative feedback loop by differentiated, non-dividing 'memory' cells captures their experimental results (6).

3. Foulds and Shen (7): Clonal Competition Inhibits the proliferation and differentiation of adoptively transferred TCR transgenic CD4 T cells in response to infection:

Foulds and Shen examined CD4⁺ T-cells response during bacterial infection by adoptive transfer of CFSE labeled monoclonal and polyclonal T cells. They find that monoclonal CD4⁺ T-cells underwent limited division relative to polyclonal CD4⁺ T-cells. They find that the limited expansion is due to the high precursor frequency of monoclonal T cells. The high amounts of the monoclonal CD4⁺ T cells also inhibited the differentiation of these cells (Fig. 3 in their paper shows different proliferation patterns for different amounts of precursor cells transferred).

4. Badovinac et al. (8): Initial T cell receptor transgenic cell precursor frequency dictates critical aspects of the CD8⁺ T cell response to infection:

Badovinac et al. show through experiments with an adoptive transfer model that high levels of CD8⁺ precursor cells squelch the endogenous response to the same epitope. They report on a 'ceiling' effect where precursor amounts are not correlated with final levels of CD8⁺ cells. Figure 1B in their paper indicates that along 4 orders of magnitude change of precursor amounts, the change in total responsive cells is less than half an order of magnitude.

5. Hataye et. al. (9): Naïve and memory CD4⁺ T cells survival controlled by clonal abundance:

Hataye et. al show through adoptive transfer model that there is an inverse relation between clonal frequency and survival of the cells. High amounts of monoclonal precursor cells transferred have a distinctively low half life (between 7-12 days) compared with low amounts of monoclonal precursor cells or polyclonal transferred cells (~100 days). Interestingly, memory cell amounts reach relatively close levels (less than an order of magnitude) though starting with more than a 4 order of magnitude difference (80 vs. 10⁵ initial monoclonal cells transferred).

6. Williams et al. (10): Rapid culling of the CD4⁺ T cells repertoire in the transition from effector to memory:

Williams et. al analyze the requirements for CD4⁺ T cell memory differentiation with adoptively transferred SMARTA T-cells. Williams et. al demonstrate that 7 days post infection total responding cell amounts are

relatively the same for all amounts of precursor cells transferred (spanning 3 orders of magnitude). Correspondingly, their expansion factor shows inverse relation with number of transferred cells (see Fig. 4 in their paper).

7. Whitmire et. al (11): Increasing the CD4⁺ T cell precursor frequency leads to competition for IFN-g thereby degrading memory cell quantity and quality:
Whitmire and colleagues show that high precursor frequency leads to a lower amount of memory cells with functional deficits. They demonstrate that competition over IFN-g signals affects the differentiation to memory cells. However, as shown at Fig. 2B in their paper, initial precursor amounts that span ~100 folds before infection yield 8 days post infection amounts differing by only ~2-4 fold.

Theoretical studies on homeostasis and differentiation processes in the immune system

In the following section we describe theoretical models and reviews not mentioned in the main text which also present mechanisms for homeostasis and suggest roles for pleiotropic signaling. Four of these studies aim to model the experimental evidences mentioned in the previous section supporting insensitivity of differentiated cell levels to progenitor cell levels. Another study suggests a different role for pleiotropic signaling in Th17-iTregs differentiation process and the final study presents a control theory analysis suggesting that for the case of cytotoxic T lymphocyte, the optimal response is a stereotypical kinetics response.

The studies and their findings are listed below:

1. Allan et al (12): Comparing Ag independent mechanisms of T cell regulation:
Allan et al use several variations of a model of cell pools (the i-th pool is cells already divided i times) to match in-vitro experimental data (containing both expansion and contraction stages). The models differ by their regulation mechanisms: autoregulation, cytokines, contact with other cells or regulation through contact with APC's. They conclude that auto-regulation or control by cytokine secretion is most probable mainly if death rate and proliferation rate both depend on cytokine levels (that are assumed to be decreasing) for both CD4⁺ and CD8⁺ cells. Mechanisms of contact dependent death are shown to be less probable. Their probability increases if these mechanisms change both rates (proliferation and death rates) and are assumed to be AICD dependent and fratricidal.

2. Kim et al. (13): Emergent group dynamics governed by regulatory cells produce a robust primary T cell response:
 Kim et al demonstrate in a recent study that programmed T cell expansion and contraction, whether based on T cell divisions or time, cannot account for the robustness of effector cell numbers to precursor cell numbers. They present a model with a negative feedback - Effector cells drive the expansion of regulatory T cells which in turn suppress effector T cells expansion by contact interactions. This negative feedback in a model simulated with delayed differential equations gives rise to a decreased dependency of effector cells on initial precursor levels: $X_{tot} \propto X_0(0)^{1/3}$.
3. Bocharov et. al (6): Feedback regulation of proliferation vs. differentiation rates explains the dependence of CD4 T-cell expansion on precursor number:
 In this recent study Bocharov et al use a multi-phase differentiation model with a negative regulation of the final phase effector cells on growth and differentiation rates of cells in previous differentiation phases. They show that using this model (with delayed response in the differential equations) results in a decreased dependency of effector cells on initial precursor levels: $X_{tot} \propto X_0(0)^{1/2}$. Their model correlates well with in-vivo experiments obtained by Quiel et. al (5).
4. Antia et al (14): The role of models in understanding CD8+ T-cell memory:
 In this review, Antia et. al discuss different models for creating memory cells. They divide the response to three main stages – expansion and contraction, homeostasis and lastly, a second response. Primary response models show that clonal expansion is differing between different epitopes (selection) where the models match proliferation and death rates achieved from BrdU and CFSE data. They discuss different differentiation of CD8+ effector cells to memory cells models and argue that ‘programmed’ cell proliferation and death rates models have better fit to the experimental results (refs 38-40 within). These models use two separated phases - exponential growth phase and exponential decay phase. They discuss the experimental finding that memory cells numbers are kept quite robust, by keeping division and death rate balanced. This balance does not need antigen presence as shown also experimentally. Lastly, they present three models for ‘maintenance’ of memory cell levels: bystander stimulation (stimulation by other antigen appearance, effects all cells), cross-reactive stimulation (stimulation by other antigen, effects only subpopulation) and homeostasis regulation. They predict that since total number of memory cells is maintained, different epitope frequencies are changed by the exposure to different pathogens.
5. Hong et. al. (15): A mathematical model for the reciprocal differentiation of T helper 17 cells and induced regulatory T cells:

Hong et al present a model for Th17 and iTregs differentiation in which the cytokine $\text{TGF}\beta$ regulates both differentiation processes from naïve CD4^+ cells. Hong et al show that their model captures similar phenotypic heterogeneity of the two key transcription factors (TF) expression levels observed in experimental studies. In particular, their model exhibits four stable steady-states of the two master TF regulators of differentiation to Th17 or iTregs (low/low, low/high, high/low and high/high). They show that their mathematical model coupled with initial cell-to-cell variability in kinetic rates exhibits the observed phenotypic diversity in cell population. When added with polarizing signals, the model can produce functionally distinct effector cell fractions as observed experimentally.

6. Van den Berg and Kiselev (16): Expansion and contraction of the cytotoxic T lymphocyte response – an optimal control approach:

In their study, van den Berg and Kiselev consider the kinetics of CTL response to intracellular pathogens. They show using control theory methods that CTL stereotypical response (as observed in several experimental studies) is the optimal kinetics to minimize the probability that a pathological symptom will occur. Their model considers pathological impacts both to pathogen and to CTL's, taking into account CTL's high killing capability. They further show that CTL kinetics are not influenced by the dose or duration of the infection, shared attributes with the stereotyped pulse of ligand we presented in the main text.

Fold change detection in the differentiation process of CD4^+ to iTregs and Th17

Here we explain in detail the derivation of the equations in Fig 5A. These equations model the fold detection mechanism suggested in the main text to occur in the differentiation process of CD4^+ cells into iTregs cells and Th17 cells.

The differentiation of CD4^+ cells to either iTregs (denoted as Y) or Th17 (denoted as X_1) requires $\text{TGF}\beta$. The inhibition of Th17 cells by iTregs cells follows from IL-10 (denoted as c_2) secretion by iTregs which inhibits the differentiation of CD4^+ cells to Th17. The incoherent feed-forward mechanism is achieved in the following way:

We assume that c_2 (IL-10) dynamics are faster than cell dynamics of differentiation and removal. Then, the dynamic equation for the production and degradation of c_2 can be evaluated at steady-state:

$$(S23) \quad \dot{c}_2 = \beta_L Y - \alpha_L c_2 = 0$$

where β_L is c_2 secretion rate and α_L is its removal rate from the medium by degradation or endocytosis. Therefore, using the quasi-steady-state assumption one has that c_2 levels are proportional to Y (iTregs) levels

$$(S24) \ c_2 = \frac{\beta_L}{\alpha_L} Y$$

As noted, c_2 inhibits $CD4^+$ differentiation to Th17 cells. The inhibition by c_2 is modeled by a Michaelis-Menten curve. Thus, the dynamic equation of the change in Th17 (X_1) levels is (compare with Fig.5, main text):

$$(S25) \ \dot{X}_1 = \beta_2 X_0 f(c) \frac{K}{K+c_2} - \alpha_2 X_1$$

where $f(c)$ is the dependence of the differentiation rate on TGF- β , here denoted as c . assuming that c_2 is produced at high levels such that $c_2 \gg K$, the Michaelis-Menten response is, to a good approximation, K/c_2 and the equation for X_1 simplifies to

$$(S26) \ \dot{X}_1 = \beta_2 X_0 f(c) \frac{K}{c_2} - \alpha_2 X_1$$

using the fact that c_2 levels are proportional to Y levels (Eq.S24), the set of dynamic equations reduces to the fold detection mechanism set of dynamic equations

$$(S27) \ \dot{X}_1 = \frac{\beta_3 X_0 f(c)}{Y} - \alpha_2 X_1$$

$$(S28) \ \dot{Y} = \beta_4 X_0 f(c) - \alpha_4 Y$$

where $\beta_3 = K \beta_2 * \alpha_L / \beta_L$ while β_4 and α_4 are the effective differentiation and removal rates of Y cells (iTregs) respectively.

An approximate analytical solution of the stereotyped pulse of the IL-27 circuit

Here we present an approximated analytical solution of the IL-27 circuit dynamic equations presented in the main text (Fig 5D-F). The dynamic equations for the dimensionless parameters X and c are:

$$(S29) \ \dot{X} = X(c - 1)$$

$$(S30) \ \dot{c} = \frac{X}{s} - \frac{1}{t_r} c$$

where s are IL-27 levels and t_r is the ratio between the degradation rates of X and c (α_1/α_2).

The system's behavior at the beginning and end of the pulse is easily analyzed: At very low concentrations of X and c (near the ending of the pulse) the equations yield that both X and c scales like e^{-t/t_r} . At the beginning of the pulse, c is very low such that $X \sim e^{-t/t_r}$ and then $c \sim t/t_r e^{-t/t_r}$.

At intermediate times, one can solve Eq. (S29) to yield:

$$(S31) \ \frac{d \log(X)}{dt} = c - 1 \rightarrow X = X_0 e^{\int c-1 dt}$$

assuming $c = t/t_r e^{-t/t_r}$ which approximates the behavior of c , one has for X and c :

$$(S32) X \sim X_0(s) e^{1 - \frac{t}{t_r} - (1 + \frac{t}{t_r})e^{-\frac{t}{t_r}}}$$

$$(S33) c \sim t/t_r e^{-t/t_r}$$

Stability analysis of the stereotyped pulse (IL-27) circuit with and without a constant production from a differentiation process

Here we discuss the stability, separatrix and the asymptotic behavior of the stereotyped pulse system presented in the main text. We also discuss this system in a different scenario where there is constant production of X cells by c_1 cytokine. This scenario assumes that a reservoir of progenitor cells, X_0 , is constantly differentiating to X_1 cells in the presence of the cytokine c_1 , and thus relieves the assumption about the sequential nature of differentiation and proliferation processes assumed in the main text.

The dynamic equations characterizing the IL-27 circuit composed of Th1 cells (X) and IL-2 cytokine (c) are given by (see section above):

$$(S34) \dot{X} = X(c - 1)$$

$$(S35) \dot{c} = \frac{X}{s} - \frac{1}{t_r} c$$

where s denotes IL-27 levels and $X(0)=K(\tau,c,X_0)*s$ is the initial condition of the cells. These equations allow scaling out IL-27 levels, such that c dynamics has a stereotyped dynamic pulse response in the sense that it is independent on IL-27 and $X(0)$ levels.

The system has two fixed points: at $X=0, c=0$ and at $X= s/t_r, c=1$. The first fixed point is a stable fixed point of the system while the second one is unstable.

The unstable (robust) fixed point at $c=1$ is part of the separatrix of the system. Initial conditions above the separatrix diverge to infinity (hyper-activity regime). Initial conditions that are below the separatrix converge to the $X=0, c=0$ fixed point.

The separatrix line can be found by integrating the following differential equation:

$$(S36) \frac{dc}{dX} = \frac{dc}{dt} / \frac{dX}{dt} = (\frac{X}{s} - \frac{1}{t_r} c) / X(c - 1)$$

We find numerically that the crossing point of the separatrix with the X axis obeys to a good approximation a simple relation:

$$(S37) X_{sep} = 1.8 s$$

Thus, the smaller s is (IL-27 levels), the smaller the threshold for hyper-activity. This result might explain why in experiments IL-27R knockout is counter intuitively hyper-active rather than inactive (17).

Next, we analyze a “perturbed” version of the IL-27 circuit, where Th1 cells are constantly produced by IL-27 acting on the naïve, $CD4^+$ cells (X_0). The dynamic equations for the system are:

$$(S38) \quad \dot{X} = X(c - 1) + s X_0$$

$$(S39) \quad \dot{c} = \frac{X}{s} - \gamma c$$

where γ is the degradation rate of c , $\gamma = 1/t_r$. These equations simulate the entire differentiation and proliferation process where initially most Th1 cells (X) are produced by the cytokine IL-27 (s) activating the differentiation of the naïve $CD4^+$ pool (X_0). As noted above, this assumes that X_0 is a reservoir of the system.

This system of equations displays different dynamics from the unperturbed system: The $X=0, c=0$ point is not a fixed point of the system. Instead, the stable fixed point moves to $X = \frac{1}{2}s (\gamma - \sqrt{\gamma(\gamma - 4X_0)})$, $c = \frac{1}{2} (1 - \sqrt{(1 - 4X_0/\gamma)})$. The second fixed point $X = \frac{1}{2}s (\gamma + \sqrt{\gamma(\gamma - 4X_0)})$, $c = \frac{1}{2} (1 + \sqrt{(1 - 4X_0/\gamma)})$ is an unstable fixed point which corresponds to the $c=1$ fixed point in the unperturbed system (Eq. S29-S30). The pulse thus does not decay back to zero, but to a nonzero steady-state. The two systems map onto one another in the limit $X_0 \rightarrow 0$, i.e. no constant production from a reservoir occurs during proliferation.

General model of robust stereotyped pulse response

Here, we generalize the conditions for mechanisms that produce a robust, stereotyped pulse that is independent on the amount of a signaling molecule, denoted c_1 . The characteristic of the robust stereotyped pulse is the ability to cancel out the effects of c_1 on the dynamic variable c_2 (the output signaling molecule). To form a pulse, the fixed point due to integral feedback must be unstable, so the dynamic trajectory first approaches it and then returns to a low or zero value. This produces a pulse in c_2 levels that decays back to zero/near zero (assumed to be a stable fixed point of the system). The general form of the dynamic equations that can produce a stereotyped pulse of c_2 are:

$$(S40) \quad \dot{X} = \phi(c_1)F\left(\frac{X}{\phi(c_1)}, c_2\right) = \phi(c_1)f\left(\frac{X}{\phi(c_1)}\right)h(c_2)$$

$$(S41) \quad c_2 = G\left(\frac{X}{\phi(c_1)}, c_2\right)$$

The integral feedback on c_2 levels is denoted as the function $h(c_2)$. Since the fixed point, c_2^* , in which $h(c_2^*)=0$, should be unstable, one has also conditions on the dynamic functions:

$$(S42) \quad f(X^*) \frac{\partial h(c_2^*)}{\partial c_2} \frac{\partial G(X^*, c_2^*)}{\partial X} > 0 \text{ or } \frac{\partial G(X^*, c_2^*)}{\partial c_2} \geq 0$$

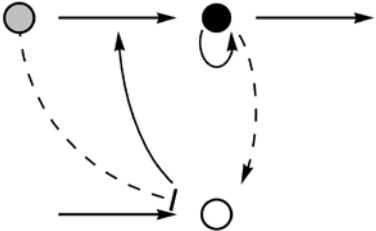
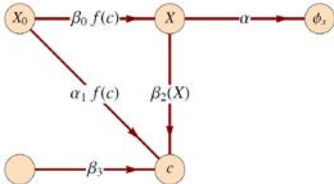
Thus, assuming the conditions in Eq. (S40-41) are met, the circuit mentioned in the main text can be generalized to cases where c_1 acts as an inhibitor of c_2 production by X ($\frac{\partial G}{\partial c_1} > 0$) while being an activator of X production ($\frac{\partial F}{\partial c_1} > 0$). In the case of a Hill function for the response to the cytokine c_1 , the condition for this mechanism to produce a robust stereotyped pulse is that $K_m^I \ll c_1 \ll K_m^A$ where K_m^A, K_m^I are the activation and inhibition half-response concentrations respectively.

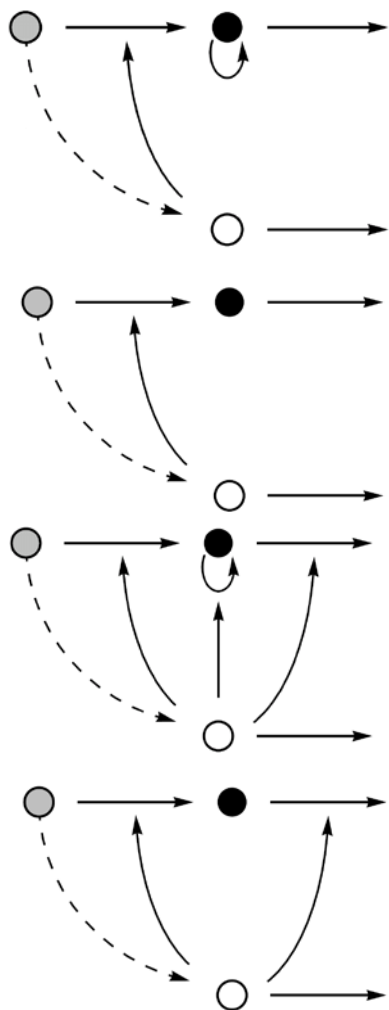
References:

1. Barkai N, Leibler S (1997) Robustness in simple biochemical networks. *Nature* 387:913-917.
2. Yi T-M, Huang Y, Simon MI, Doyle J (2000) Robust perfect adaptation in bacterial chemotaxis through integral feedback control. *Proceedings of the National Academy of Sciences of the United States of America* 97:4649 -4653.
3. El-Samad H, Goff JP, Khammash M (2002) Calcium Homeostasis and Parturient Hypocalcemia: An Integral Feedback Perspective. *Journal of Theoretical Biology* 214:17-29.
4. Whitmire JK, Benning N, Whitton JL (2006) Precursor frequency, nonlinear proliferation, and functional maturation of virus-specific CD4+ T cells. *J. Immunol* 176:3028-3036.
5. Quiel J et al. (2011) Antigen-stimulated CD4 T-cell expansion is inversely and log-linearly related to precursor number. *Proc. Natl. Acad. Sci. U.S.A* 108:3312-3317.
6. Bocharov G et al. (2011) Feedback regulation of proliferation vs. differentiation rates explains the dependence of CD4 T-cell expansion on precursor number. *Proc. Natl. Acad. Sci. U.S.A* 108:3318-3323.
7. Foulds KE, Shen H (2006) Clonal competition inhibits the proliferation and differentiation of adoptively transferred TCR transgenic CD4 T cells in response to infection. *J. Immunol* 176:3037-3043.

8. Badovinac VP, Haring JS, Harty JT (2007) Initial T cell receptor transgenic cell precursor frequency dictates critical aspects of the CD8(+) T cell response to infection. *Immunity* 26:827-841.
9. Hataye J, Moon JJ, Khoruts A, Reilly C, Jenkins MK (2006) Naive and memory CD4+ T cell survival controlled by clonal abundance. *Science* 312:114-116.
10. Williams MA, Ravkov EV, Bevan MJ (2008) Rapid culling of the CD4+ T cell repertoire in the transition from effector to memory. *Immunity* 28:533-545.
11. Whitmire JK, Benning N, Eam B, Whitton JL (2008) Increasing the CD4+ T cell precursor frequency leads to competition for IFN-gamma thereby degrading memory cell quantity and quality. *J. Immunol* 180:6777-6785.
12. Allan MJ, Callard R, Stark J, Yates A (2004) Comparing antigen-independent mechanisms of T cell regulation. *Journal of Theoretical Biology* 228:81-95.
13. Kim PS, Lee PP, Levy D (2009) Emergent Group Dynamics Governed by Regulatory Cells Produce a Robust Primary T Cell Response. *Bull. Math. Biol.* 72:611-644.
14. Antia R, Ganusov VV, Ahmed R (2005) The role of models in understanding CD8+ T-cell memory. *Nat Rev Immunol* 5:101-111.
15. Hong T, Xing J, Li L, Tyson JJ (2011) A mathematical model for the reciprocal differentiation of T helper 17 cells and induced regulatory T cells. *PLoS Comput. Biol.* 7:e1002122.
16. Vandenberg H (2004) Expansion and contraction of the cytotoxic T lymphocyte response?an optimal control approach. *Bulletin of Mathematical Biology* 66:1345-1369.
17. Villarino A et al. (2003) The IL-27R (WSX-1) Is Required to Suppress T Cell Hyperactivity during Infection. *Immunity* 19:645-655.

Table S1: Five classes of circuit topologies can show robustness to progenitor cells levels.

Circuits	Equations	Conditions for robustness	Example Circuit
<div></div> <p>Total number of topologies: 4 (all shown in Fig 3 in the text)</p>	$\dot{X}_1 = \beta_0 f(c) X_0 + (\beta - \alpha) X_1$ $\dot{c} = \beta_3 + \beta_2(X_1) - \alpha_1 f(c) X_0$	The same function $f(c)$ describes signaling and endocytosis.	<div>$\dot{X}_1 = \beta_0 f(c) X_0 - \alpha X_1$$\dot{c} = \beta_3 + \beta_2(X_1) - \alpha_1 f(c) X_0$</div>



Total number of topologies: 4

$$\dot{X}_1 = \beta_0 f(c) X_0 + (\beta - \alpha) X_1$$

$$\dot{c} = \beta_1(X_0) - \gamma c$$

$$\dot{X}_1 = \beta_0 f(c) X_0 + (\beta(c) - \alpha(c)) X_1$$

$$\dot{c} = \beta_1(X_0) - \gamma c$$

$$f\left(\frac{\beta_1(X_0)}{\gamma}\right) \sim \frac{1}{X_0}$$

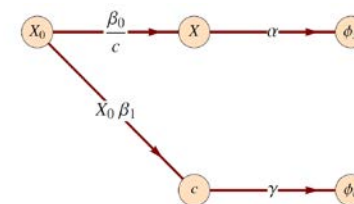
Or

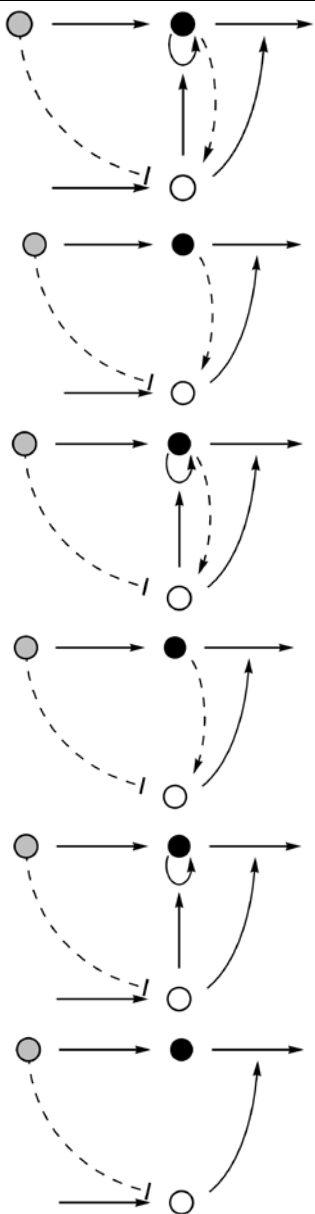
$$f\left(\frac{\beta_1(X_0)}{\gamma}\right) X_0 \sim \alpha, \beta\left(\frac{\beta_1(X_0)}{\gamma}\right)$$

Here, c effect on differentiation goes as a Michaelis-Menten-like (MM) term, approximated as $1/c$, appropriate when $c \gg c_{50}$.

$$\dot{X}_1 = \frac{\beta_0 X_0}{c} - \alpha X_1$$

$$\dot{c} = \beta_1 X_0 - \gamma c$$





Total number of topologies: 6

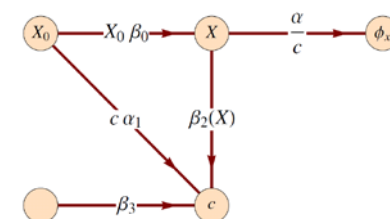
$$\begin{aligned}\dot{X}_1 &= \beta_0(X_0) + (\beta(c) - \alpha(c))X_1 \\ \dot{c} &= \beta_3 + \beta_2(X_1) - \alpha_1 f(c)X_0\end{aligned}$$

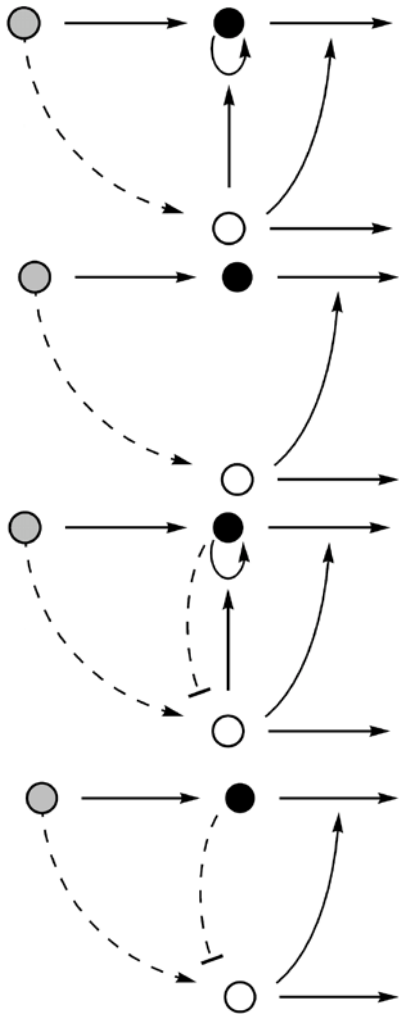
$$\alpha, \beta \left(f^{-1} \left(\frac{\beta_3 + \beta_2(X_1)}{\alpha_1 X_0} \right) \right) \sim \beta_0(X_0)$$

Here, c inhibits X_1 removal, with MM kinetics approximated as $1/c$ (appropriate when $c \gg c_{50}$). Uptake of c by X_0 is linear in c .

$$\dot{X}_1 = \beta_0 X_0 - \frac{\alpha}{c} X_1$$

$$\dot{c} = \beta_3 + \beta_2(X_1) - \alpha_1 c X_0$$





Total number of topologies: 4

$$\dot{X}_1 = \beta_0(X_0) + (\beta(c) - \alpha(c))X_1$$

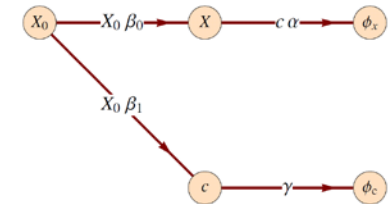
$$\dot{c} = \beta_1(X_0) - \alpha_2 f(c)X_1 - \gamma c$$

- a) $\alpha_2 f(c) = 0$ &
 $\alpha, \beta \left(\frac{\beta_1(X_0)}{\gamma} \right) \sim \beta_0(X_0)$
- b) $f(c) \sim c$ &
 $\alpha, \beta \left(\frac{\beta_1(X_0)}{\gamma + \alpha_2 X_1} \right) \sim \beta_0(X_0)$

Here, c activation of X_1 removal is linear.

$$\dot{X}_1 = \beta_0 X_0 - \alpha c X_1$$

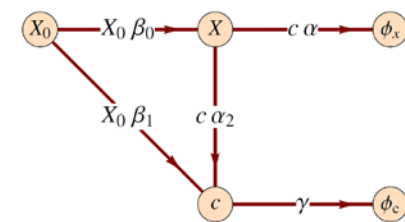
$$\dot{c} = \beta_1 X_0 - \gamma c$$



Here, both uptake of c and X_1 removal are linear in c, in addition to c degradation

$$\dot{X}_1 = \beta_0 X_0 - \alpha c X_1$$

$$\dot{c} = \beta_1 X_0 - \alpha_2 c X_1 - \gamma c$$



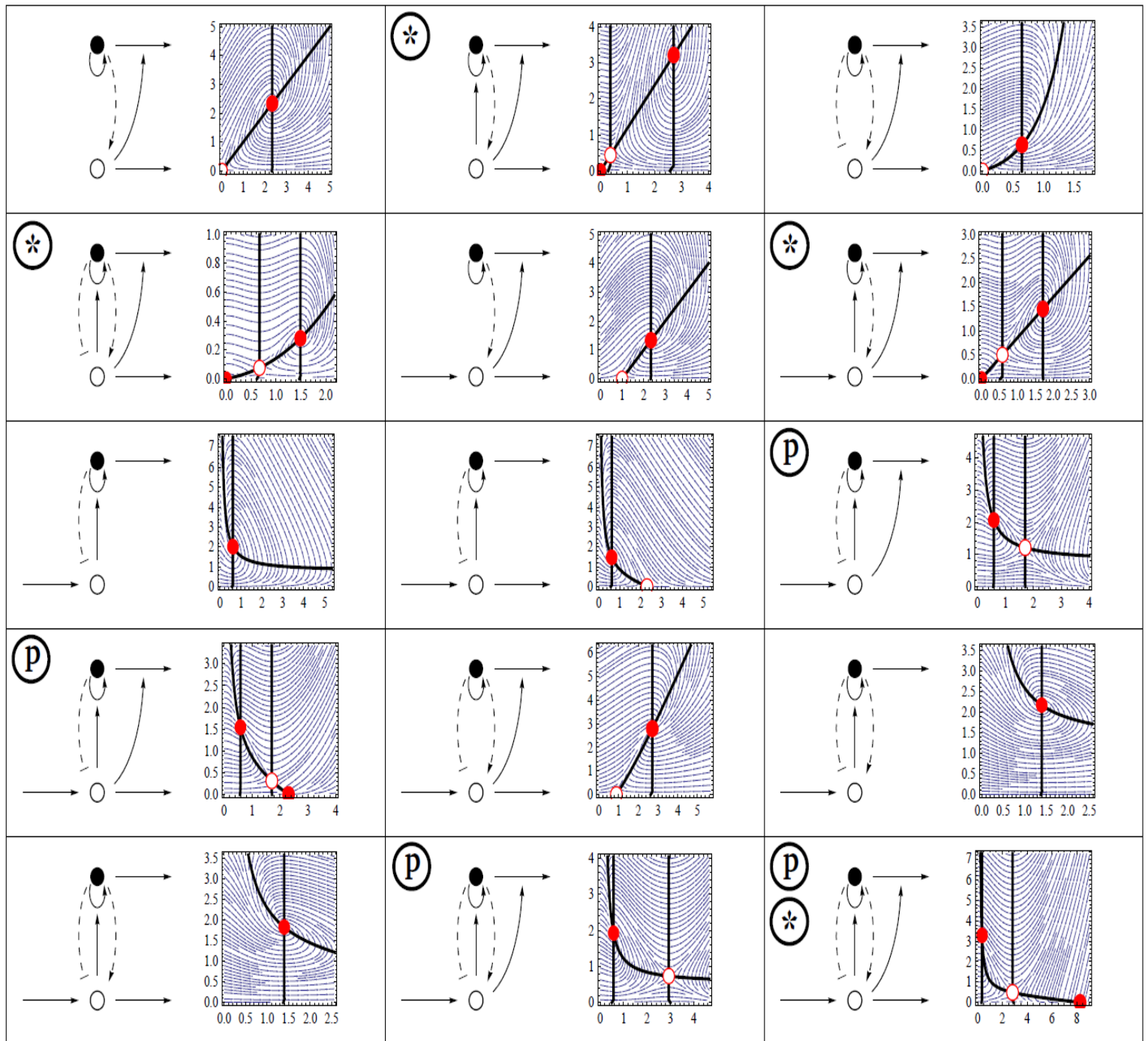


Figure S1: **Circuit topologies and dynamic phase space with a stable ON state which is independent on initial conditions.** Shown are all 15 topologies with one cell type and one ligand that exhibit a stable ON state. Shown also are the phase space (x axis is ligand levels and y axis is cell levels), nullclines, flow lines and fixed points: full and open circles represent stable and unstable fixed points respectively. Of these, four topologies also show a stable OFF state (marked with star). Four of the topologies exhibit a ligand pulse before reaching the ON state which is characterized by high cell amounts and low ligand levels (marked with p). All topologies with a pleiotropic ligand are indicated with a circle. The functional form of the circuit interactions are: cell removal: $\alpha(c) = 1 + c$, cell proliferation: $\beta(c) = \frac{c^2}{1+c^2}$ and ligand uptake: $f(c) = \frac{c}{c+1}$. For legend, see Fig 3 in the main text.

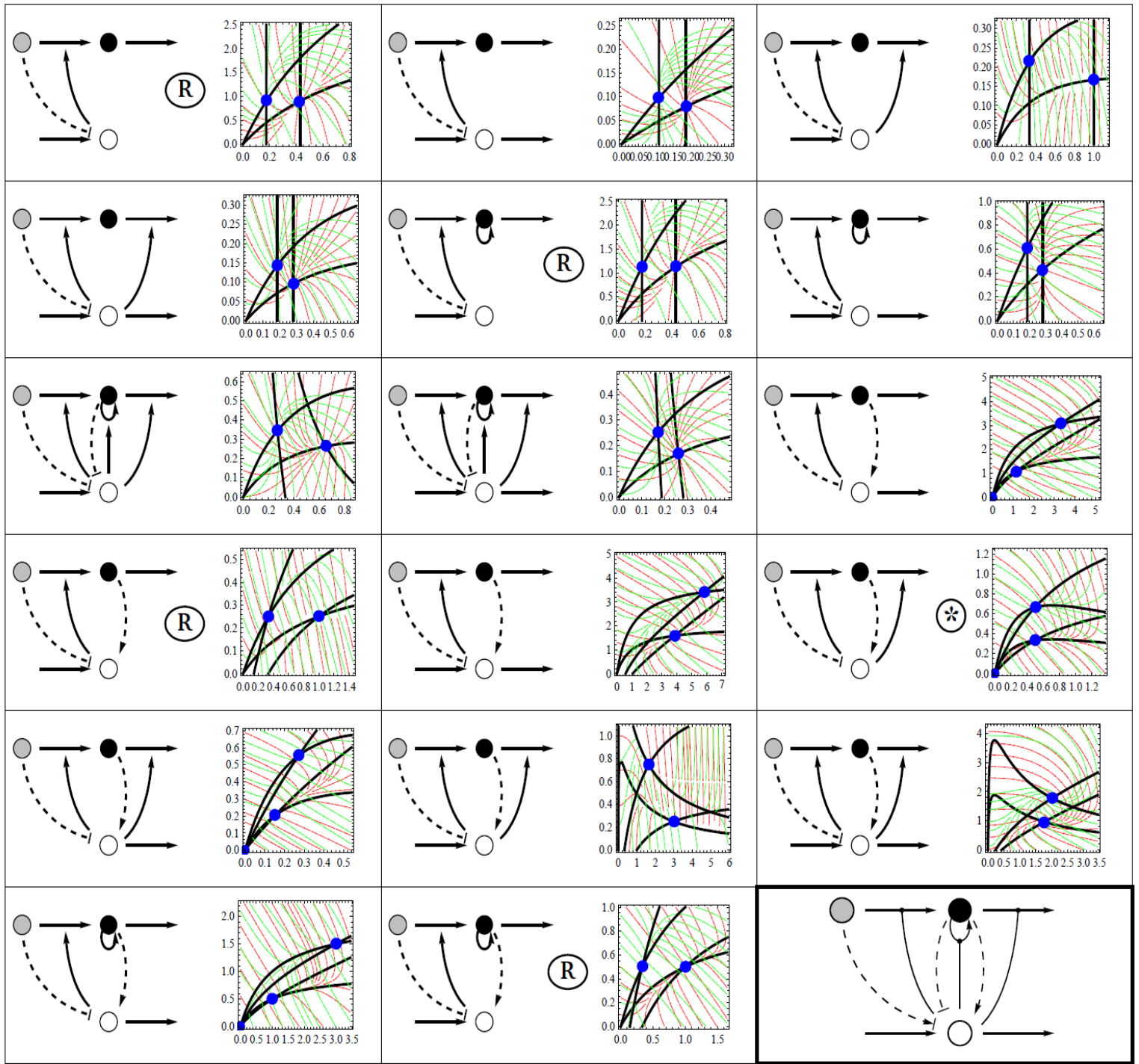


Figure S2: Circuit topologies and dynamic phase space of circuits of two-cell types and one ligand.

Analysis of a sample of circuits out of the 280 connected circuit topologies of two cell types and one ligand. Shown are the circuit topology and the circuit nullcline, steady-state and flow lines, for two progenitor cell levels: $X_0=1$ and $X_0=2$ (green and red flow lines and steady state points respectively). The four circuits that yield a steady-state solution which is independent of progenitor levels are marked by R – note that the steady state point moves parallel to the X axis. These circuits employ differentiation and endocytosis with the same functional form. Another circuit (marked in an asterisk) is shown to have ligand levels that are independent of progenitor levels – steady state moves parallel to the Y axis. All other circuits show dependence on progenitor cells for both differentiated cell levels and ligand levels. The functional form of the circuits' interactions was chosen to be - cell removal: $\alpha(c) = 1 + c$, cell proliferation: $\beta(c) = \frac{c^2}{1+c^2}$ and ligand uptake by both cell types: $f(c) = \frac{c}{c+1}$. **Inset** (bottom right, highlighted), the maximally connected interaction scheme of two cell types, a progenitor cell type that differentiates, and a ligand. For legend see Fig 3 in the main text.